Geophysical Research Letters

RESEARCH LETTER
10.1002/2015GL065173

Key Points:
- Observations show wind stress direction in typhoon impacted by wavefield
- Stress direction in typhoon is misaligned up to 35° from the wind direction
- Wind sea and swell behind typhoon lack separation in frequency and direction

Correspondence to:
H. Potter,
henry.potter.ctr@nrl.navy.mil

Citation:
Potter, H., C. O. Collins III, W. M. Drennan, and H. C. Graber (2015), Observations of wind stress direction during Typhoon Chaba (2010), *Geophys. Res. Lett.*, *42*, 9898–9905, doi:10.1002/2015GL065173.

Received 9 JUL 2015
Accepted 20 OCT 2015
Accepted article online 9 NOV 2015
Published online 21 NOV 2015

Observations of wind stress direction during Typhoon Chaba (2010)

Henry Potter[1], Clarence O. Collins III[2], William M. Drennan[3], and Hans C. Graber[3]

[1]Remote Sensing Division, Naval Research Laboratory, Washington, DC, USA, [2]Oceanography Division, Naval Research Laboratory, Hancock County, Mississippi, USA, [3]Rosenstiel School of Marine and Atmospheric Science, University of Miami, Miami, Florida, USA

Abstract Direct flux measurements of stress direction taken at the ocean surface during Typhoon Chaba (2010) over 3 days are examined for wind speeds between 12 and 26.5 m s^{-1}. Results show stress deviated up to 35° from the wind direction and resided predominantly between the wind and peak wave directions in both bimodal and unimodal seas. Off-wind stress angle was most pronounced in Chaba's wake where wind sea and swell created an apparent unimodal system with narrow directional spread. These conditions lasted 2 days during which the stress direction was midway between the wind and wave directions. The implications for tropical cyclone forecasting are discussed.

1. Introduction

Surface wind stress facilitates the exchange of momentum at the air-sea interface. At high wind speeds, momentum exchange is a key component of the tropical cyclone (TC) life cycle because it drives wave growth, which modifies surface drag [*Holthuijsen et al.*, 2012] and mixes the ocean, bringing cooler water to the surface which reduces heat fluxes [e.g., *Fisher*, 1958] and alters boundary layer stability, which has been linked to increased heat and moisture into the eyewall [*Lee and Chen*, 2014]. Accurate understanding of the wind stress is essential for modeling of TC as well as storm surge and wave prediction [e.g., *Moon et al.*, 2004; *Ooyama*, 1969].

Numerous studies have investigated the magnitude of the wind stress [e.g., *Potter*, 2015; *Smith*, 1980], given by

$$\vec{\tau} = \rho\left[\left(-\overline{u'w'}\right)\vec{\imath},\ \left(-\overline{v'w'}\right)\vec{j}\right] \tag{1}$$

where $\vec{\tau}$ is the wind stress vector, ρ is the air density, $\vec{\imath}$ and $\vec{j}$ are unit vectors along and perpendicular to the mean wind direction, and u, v, and w are the down-wind, cross-wind, and vertical components of wind velocities, respectively. An overbar indicates time average of order 30 min, and a prime denotes a component which fluctuates from the mean ($\overline{u'} = \overline{v'} = \overline{w'} = 0$). The direction of the wind stress with respect to the mean wind is

$$\theta = \arctan\left[\left(-\overline{v'w'}\right)/\left(-\overline{u'w'}\right)\right]. \tag{2}$$

Positive angles correspond to the stress vector oriented to the right of the wind direction.

Monin-Obukhov Similarity Theory (MOST) [*Monin and Obukhov*, 1954] assumes that the stress vector is aligned with the wind vector. Some early studies [e.g., *Large and Pond*, 1981; *Geernaert et al.*, 1986] followed MOST and assumed that the crosswind stress component was insignificant compared to the downwind component, and neglected it. Other studies [e.g., *Smith*, 1980] found that $-\overline{v'w'}$ was large enough to alter the stress direction away from the direction of the mean wind. Nonalignment of the near-surface wind and stress directions have since been attributed to surface currents or current shear [e.g., *Drennan and Shay*, 2006; *Zhang et al.*, 2009], and waves. *Geernaert et al.* [1993] showed that in mixed seas where both swell and wind sea are present, a component of the crosswind contribution to the momentum flux exists in the frequency band of the swell system. This manifests itself as turning of the wind stress in the direction of the long waves, especially if swell is steep. For wind speeds up to ~14 m s^{-1}, *Rieder et al.* [1994] also reported that stress direction lay between the direction of the wind and the long waves, particularly for winds over 8.6 m s^{-1}. *Grachev et al.* [2003] proposed a dynamic link between the stress direction and waves, showing that the stress direction is the vector sum of the pure shear stress, the wind-wave induced stress aligned with the direction of the pure wind sea waves, and the swell.

The stress angle has been the subject of renewed interest lately, due to its importance in ocean-wave-atmosphere coupled models, particularly those developed for TC modeling. The model of *Moon et al.* [2004] predicted that the off-wind stress direction in TC lies between the mean wind and dominant wave directions, echoing low wind speed observations, and was most pronounced in the TC front-left quadrant, which had the largest directional difference between dominant waves and wind. The authors reported that the stress angle never exceeded a few degrees because the waves which carry most of the stress are in the equilibrium range aligned with the wind, while dominant waves which are misaligned from the wind support little stress. The authors explicitly neglected swell which counter the waves, claiming that they have little effect on the stress during TCs. *Chen et al.* [2013], whose model allowed for the inclusion of swell waves, reported relative stress angles up to 25°, with the highest angles near the eyewall, and to the left of the storm track. *Reichl et al.* [2014] used two approaches to model the wind stress and found that the parameterization which introduced a contribution from the crosswind swell increased the off-wind stress angle. This angle was more enhanced during lower wind speeds, for faster translating TCs, near the center, and to the left of the storm where swell was present. Misalignment angle rarely exceeded 5° and never 10°.

With previous stress direction measurements made at low to moderate wind speeds and none recorded at the surface in TCs, there remains a dearth of knowledge with which to validate TC models. Observations of stress in TCs are sparse and most are indirect, relying on dropsonde profiles of wind extrapolated to the surface [e.g., *Powell et al.*, 2003]. To our knowledge only *Zhang* [2007] and *Zhang and Drennan* [2012], using airplane measurements during the Coupled Boundary Layer Air-Sea Transfer Experiment have reported stress directions in TCs, finding them to be nonzero. However, *Zemba and Friehe* [1987] showed that off-wind stress angle increases systematically with height due to Ekman effects, so it is not clear if the Zhang and Drennan findings, based on data collected 60-400 m above the surface, were due to TC dynamics. No near-surface measurements of stress direction at high wind speeds have ever been reported.

This is one of the largest knowledge gaps in understanding moderate to high wind speed momentum transfer at the sea surface. This paper fills this gap by reporting direct observations of stress direction during typhoon Chaba (2010) for wind speeds up to 26.5 m s^{-1}. Measurements made over 3 days are examined and discussed in relation to the wavefield. The results of this study will lead to better momentum flux parameterizations and more accurate TC models.

2. Data Collection

Data were collected during the 2010 Impact of Typhoons on the Ocean in the Pacific (ITOP) experiment from an Extreme Air-Sea Interaction (EASI) buoy [*Drennan et al.*, 2014]. EASI was surface moored in the Philippine Sea 126.96°E, 21.23°N, approximately 750 km east of Taiwan with a depth of ~5500 m and equipped to measure air-sea fluxes of momentum, heat, and mass as well as mean meteorological and oceanographic parameters. A Gill R2A sonic anemometer, positioned 5.45 m above mean sea level, recorded wind speed and direction at 20 Hz, which was stored on a below-deck data acquisition system. EASI's motion, recorded by two full motion packages, was used to motion correct the sonic data following *Anctil et al.* [1994] and also enabled EASI to operate as a heave-pitch-roll buoy [*Longuet-Higgins et al.*, 1963]. Of interest here is the calculation of mean wave direction at the peak frequency, $\theta(f_p) = \arctan(B_1(f_p)/A_1(f_p))$, and directional spread at the peak, $\sigma(f_p) = 2\left(1 - \sqrt{A_1^2(f_p) + B_1^2(f_p)}\right)^{1/2}$, where A_1 and B_1 are the first directional moments calculated from the co-spectra and quadrature-spectra of buoy motion [*Kuik et al.*, 1988] and f_p is the peak frequency of the waves based on the one-dimensional wave spectrum. Note that $\theta(f_p)$ is essentially an energy weighted mean direction, which may not correspond to the actual peak in frequency-direction space. *Collins et al.* [2014a, 2014b] determined that $\theta(f_p)$ was accurate within ±10° and provide extensive information about EASI as a wave buoy. Further information about the ITOP experiment can be found at *Potter et al.* [2015] and *D'Asaro et al.* [2014].

Data were processed in runs of 30 min. Each run was analyzed for spikes in u, v, and w. Isolated spikes greater than 4 standard deviations from their respective means were interpolated through. Overall, spikes proved rare, the highest wind speed runs averaged about 20 isolated spikes. After applying careful quality control measures, mean wind speeds were raised to their 10 m neutral equivalent values U_{10N} using MOST [*Monin and Obukhov*, 1954].

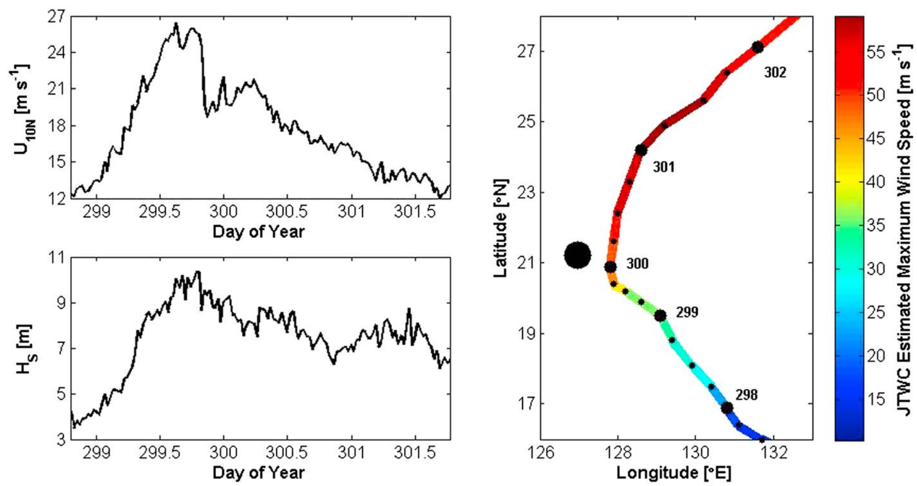

Figure 1. (top left) U_{10N} (bottom left) H_S recorded during Typhoon Chaba during the period of interest (DOY 298.8–301.8). Also shown is Chaba's JTWC estimated storm track and maximum wind speed (right). Each dot on the track marks storm location every 6 h and numbers show DOY at 00UTC. EASI's location is denoted by the large isolated black dot.

We assume that our stress angle data at 5.45 m are representative of conditions at 10 m. While anemometer failure prevented us from having stress angle measurements from multiple heights during ITOP, we refer to unpublished data from a 2003 experiment in the Baltic [*Högström et al.*, 2008]. Here sonic anemometers were deployed at 5.3 and 2.56 m above mean sea level on an Air-Sea Interaction Spar buoy. Based on over 600 h of data with wind speeds over 5 m s^{-1} (as here), the mean difference between the stress angles at the two heights was 2.11° (standard deviation 10.33°). There was no systematic effect of this difference on wind speed, stress angle, wave age, or wave height. Hence, we are confident that the stress angle values at 5.45 m are representative of those at 10 m.

3. Typhoon Chaba

Here we examine data collected during Typhoon Chaba, which had the highest wind speeds recorded on EASI during the experiment. Because of our interest in stress direction under a TC and in high wind speeds, we restrict analysis between day of year (DOY) 298.8 and 301.8 during which U_{10N} was above 12 m s^{-1}and reached a maximum of 26.5 m s^{-1}. During that period, Chaba ranged from a category one typhoon to category four and passed within two radii of maximum winds (RMW) of EASI.

Chaba's storm track and estimated maximum wind speeds from the Joint Typhoon Warning Center (JTWC) [*Angrove and Falvey*, 2010] are shown in Figure 1 with U_{10N} and significant wave height H_S. Chaba approached EASI from the southeast moving at ~3 m s^{-1}. On DOY 299.75, while still on EASI's east, Chaba turned and headed north, passing closest to EASI on DOY 300 when its RMW was within 49 km. At that time, JTWC estimated Chaba had a maximum wind speed of 49 m s^{-1}, which increased to 59 m s^{-1} over the following 48 h as it propagated northeastward while its pace increased from ~3 to ~7 m s^{-1}.

4. Wind, Wave, and Stress Directions

Figure 2 shows the wind direction (blue), wave direction at the peak frequency (green), and stress direction (magenta) plotted in a typhoon reference frame. The distance from EASI to Chaba at the time of each measurement normalized by JTWC estimated RMW. Note that no measurements were made within one RMW and few were made to Chaba's right.

In an anticlockwise rotating sense, the wind direction was generally ahead of the peak wave and stress directions. Greatest off-wind stress directions were recorded from DOY 300.5 to 301.3 when EASI was 5–12 RMW behind Chaba. During that time, off-wind stress angle remained above 22° and reached maximum of 35°on DOY 300.8. Stress direction was predominantly between the wind and peak waves, this delineation was consistent

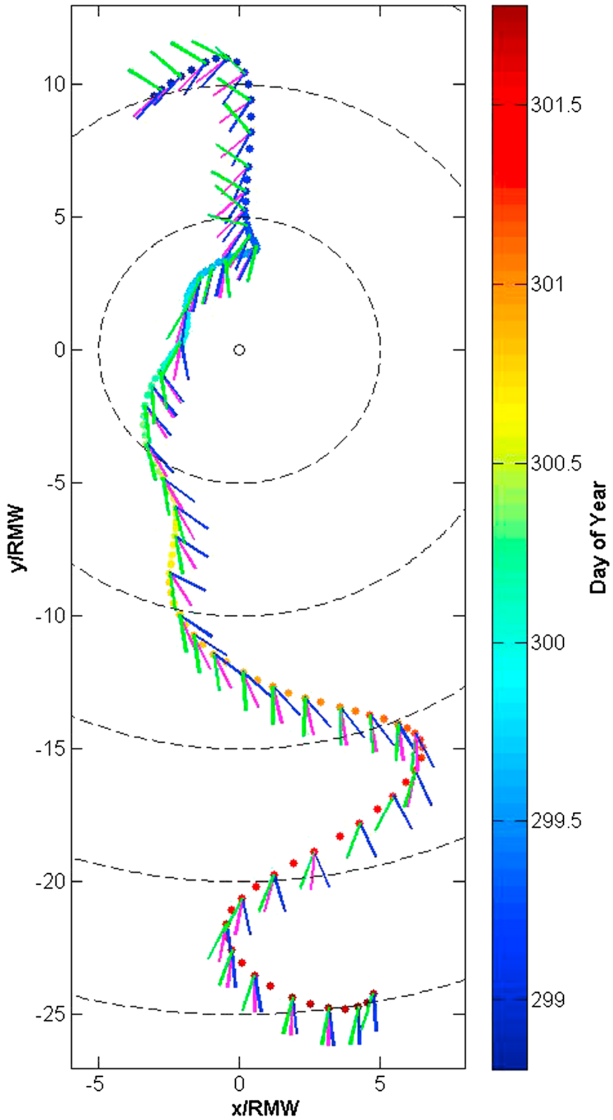

Figure 2. Mean direction of wind (blue), stress (magenta), and waves at peak frequency (green) during Chaba. The figure is plotted in typhoon reference frame and distance is normalized by RMW. Concentric circles show 5, 10, 15, 20, and 25 RMW. The dots show the location of EASI in relation to Chaba's RMW every 30 min; dot colors denote DOY. For clarity directions are only displayed every 1–2 h.

for measurements made after DOY 299.7 when EASI was no longer directly ahead of Chaba. This is shown in Figure. 3

We have pinpointed periods of interest (A, B, C) in Figure 3, which presents unique wind, stress, and wave directional characteristics. In period A, measurements were made ahead of Chaba and show dominant waves ~100° from the wind direction, the result of a swell system generated by, and moving ahead of, Chaba. Period B lasted from DOY 299.3–299.9. During that time, the wind seas were dominant, the directional spread was large, and the wind and stress directions were approximately aligned. On DOY 299.7—when Chaba turned and headed north—the stress became positioned between the wind and peak wave directions where it remained for approximately 2 days. During period C EASI moved from being on Chaba's weak side to behind the typhoon. This coincided with a rapid shift in wind, stress, and peak wave directions, and a reduction in directional spread.

During the passage of Chaba the stress direction at EASI was prevalently to the right of the wind. The misalignment of the stress from the wind was often akin to a misalignment between the wind and peak wave directions. We explore this relationship by plotting off-wind stress angle versus off-wind wave angle (Figure 4). Periods from Figure 3 are identified. The correlation between the off-wind stress and off-wind peak wave directions during C is illustrated by a best fit line, which shows the stress resided approximately midway between the wind and peak wave directions ($r = 0.6$).

5. Discussion

Next, we take a closer look at the wavefields for periods A, B, and C in order to evaluate any correlation to the off-wind stress angle during Chaba. Figure 5 shows snapshots of the 2-D wave spectra for periods A, B, and C. Each panel is 2 h averaged spectra plotted in log scale.

During period A the wavefield was bimodal. Measurements were made in the front-left quadrant of Chaba where swell was dominant, leading to a large off-wind peak wave angle. Correlation between off-wind peak wave and stress angles during this period ($r = 0.55$) suggests that the swell contributed to stress turning, which deviated up to 20° from the wind direction. Previous studies have also shown swell turning stress of similar magnitude (c.f. Figure 6 of *Rieder et al.* [1994]) but in response to considerably more acute off-wind swell directions. Throughout B the wind sea energized rapidly. During intensification, the dominant wave

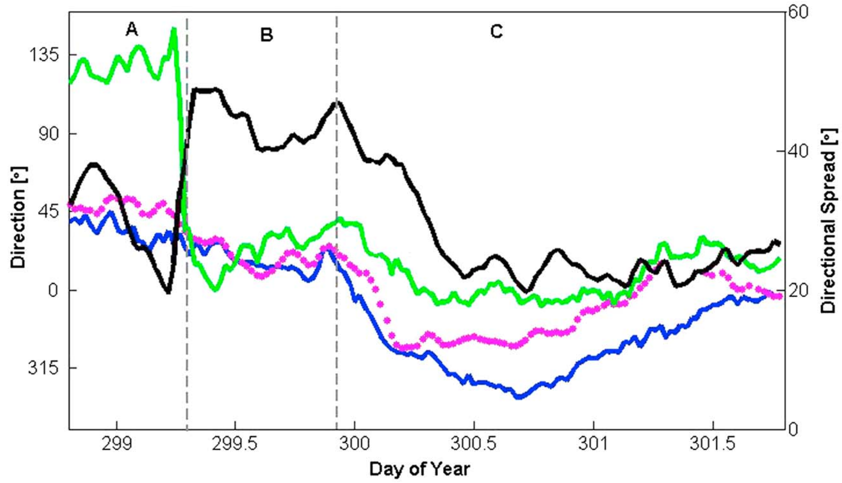

Figure 3. Time series of wind direction (blue), stress direction (magenta), mean (energy weighted) wave direction at the peak frequency (green), and directional spread at the peak (black). A, B, and C relate to specific periods referred to in the text. Wave direction has been smoothed with a five point moving average.

direction bounced back and forth between the wind sea and the swell until the wind sea, propagating SSE, was established as the dominant system. It also shifted to ~0.1 Hz, acquiring approximately the same frequency as the westward propagating swell, and developing large directional spread.

As the wavefield evolved (Figure 5c) the swell and wind sea become indistinguishable in direction and frequency. This newly established wavefield was unimodal with the peak frequency to the right of the wind direction and the directional spread significantly reduced. By virtue of being in a rotating system both locally generated swell and wind sea components must have existed; however, there was a lack of separation in frequency and direction so they could not be isolated. The swell-like component would have been right of the wind sea, but being recently generated, would have possessed wind sea qualities and is better characterized as a noncoherent wind sea than traditional swell. Our observations indicate that waves under TC are very complex, and we acknowledge wave energy existed outside this spectral peak, but because it was so dominant, we feel justified referring to the wavefield as unimodal during this period.

The transition from a bimodal to unimodal sea coincided with EASI shifting from ahead of Chaba to its weak side. Over the following 12 h rapid parallel swings in the wind, stress, and peak wave directions occurred as

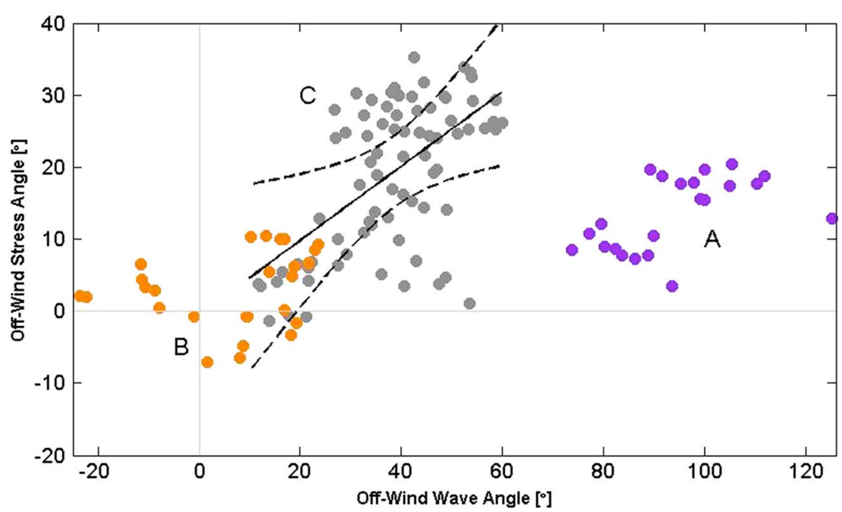

Figure 4. Off-wind stress angle versus off-wind wave angle. Periods A (purple), B (orange), and C (grey) are defined in Figure 3. Period C has been fitted with a line of best fit ($r = 0.6$); dashed lines show 95% confidence interval.

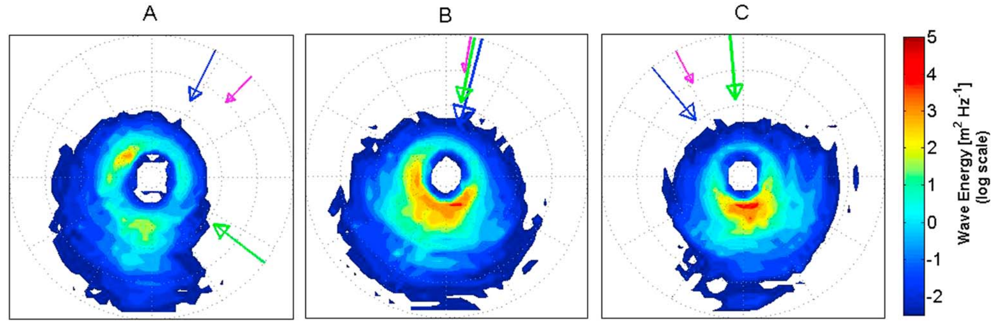

Figure 5. 2-D wave spectra for selected periods during Chaba as highlighted in Figure 3. Each panel is a representative 2 h averaged spectra plotted in log scale, and concentric circles are frequency bands from 0.1 (inner) to 0.5 Hz (outer) for waves traveling outward from the center. Arrows point in wind direction (blue), mean wave direction at the peak frequency (green), and stress direction (magenta). The wind and wave arrows have length equal to their velocity, with each frequency band representing 10 m s^{-1}. Stress arrows have a length normalized to one frequency band. North and east are the top and right of the plots, respectively.

Chaba passed EASI while remaining within three RMW of the buoy. By DOY 299.9 the waves were becoming more organized through dispersion as the storm moved away and the waves traveled increasing distances before reaching EASI. This manifests in decreasing directional spread, which drops to 50% of the peak TC value. The resulting wavefield was well organized and persisted for about 40 h (Figure 5c). The uniformity of the wave characteristics and correlation between the off-wind wave and off-wind stress directions during period C (recall Figure 4) suggests that the unimodal wavefield generated by Chaba impacted the stress direction by turning it away from the mean wind and toward the peak wave direction. Previous studies have shown that the stress direction can be turned by the swell at low wind speeds [e.g., *Geernaert et al.*, 1993], but this has not been confirmed in TC conditions. Evidence suggests that the very steep noncoherent wind sea contributed to stress turning during Chaba.

The scatter in Figure 4D suggests that stress direction could also have been influenced by other processes; subsequently, we now consider the potential influence of surface currents and temporal nonstationarity.

Surface currents 1–2 m s^{-1} have been recorded in TC [*Withee and Johnson*, 1976]. At these speeds, currents have been shown to impact stress direction, [e.g., *Drennan and Shay*, 2006], although upper ocean transport is much slower on the left side of a TC [e.g., *Price*, 1981]. Despite current velocity being influenced by wind speed [e.g., *Smith et al.*, 1992], no correlation was found between the off-wind stress angle and the wind speed, or the proximity of EASI to storm center. This suggests that any stress turning by surface currents likely had nominal influence during the periods in question.

Quanduo and Komen [1993] showed that nonstationary events, due to different rates of turning for the wind and wind sea directions, may lend themselves to differences between the wind and stress vectors. Here we test the level of stationarity during Chaba using the sampling error of the turbulent flux estimate. This is based on the premise that, during stationary conditions, the sampling error in the flux estimate is consistent with observed variability. The flux variability [e.g., *Sreenivasan et al.*, 1978] is estimated by

$$\frac{\sigma_F}{F'} = \alpha_F z^{1/2} U^{-1/2} \Upsilon^{-1/2}. \tag{3}$$

F' is the mean flux over the study period, σ_F is the standard deviation of the flux, Υ is sampling interval, and α_F is a constant = 6.4 [*Sreenivasan et al.*, 1978]. When applied to the 2 h during peak measured wind speeds, expected sampling variability was 0.073. This reasonably well predicted the observed variability of 0.088. The result here is of the same order and so conditions were essentially stationary. Similarly, during the Gas Exchange Experiment when conditions were considered largely stationary, the estimated variability of 0.16 was thought to be a good a prediction of the measured variability of 0.18 [*Drennan et al.,* 2007]. It should also be noted that this test was used to assess stationarity on the time scale of 2 h, but in this study data are processed over periods of 30 min and only assumes stationarity on that scale.

6. Conclusion

We report the first direct flux measurements of stress direction in a typhoon. Measurements made during Typhoon Chaba with wind speeds from 12 to 26.5 m s^{-1} showed stress deviated up to 35° from the wind direction. A positive correlation between the directions of the stress and peak waves occurred over ~2 days when measurements were made behind Chaba, while the wavefield was unimodal, i.e., there was lack of frequency separation between the wind sea and locally generated swell, and the directional spread was small. Results indicate that waves contributed to stress being misaligned from the mean wind direction. The off-wind stress angle reported here is much greater than previously anticipated by TC models or could be inferred from studies with much lower wind speeds. It was also found that stress direction is turned significantly in unimodal seas, which has not previously been reported, as well as bimodal. Results should be incorporated into TC models by modifying surface layer parameterization of stress direction in relation to the wavefield. This will result in more accurate prediction of TC track and intensity and have critical implications for risk assessment of landfalling TC.

Acknowledgments

ITOP data are freely available from EOL data archives at data.eol.ucar.edu. ITOP was funded by ONR under grant N0014-09-1-0392. We thank this agency for their support. We acknowledge additional support from NSF (OCE-0526442) for the development of the EASI buoy and ONR (DURIP N00014-09-0818) for funding construction of the second EASI buoy. We are also grateful for contributions of Mike Rebozo, Rafael Ramos, and Neil Williams at RSMAS, the WHOI mooring group led by John Kemp, and for the support and assistance provided by the captains and crew of the R/V *Roger Revelle*. We thank an anonymous reviewer for questioning our assumption of equal stress directions at different measurement heights and our interpretation of the wavefield. This research was conducted in part thanks to Henry Potter's NRC research associateship at the Naval Research Laboratory, Washington DC, and Clarence O. Collins' ASEE post-doctoral fellowship at the Naval Research Laboratory, Stennis Space Center.

References

Anctil, F., M. A. Donelan, W. M. Drennan, and H. C. Graber (1994), Eddy-correlation measurements of air-sea fluxes from a discus buoy, *J. Atmos. Oceanic Technol.*, *11*, 1144–1150, doi:10.1175/1520-0426(1994)011,1144:ECMOAS.2.0.CO;2.

Angrove, M. D., and R. J. Falvey (2010), Annual tropical cyclone report 2010, U.S. Naval Maritime Forecast Center/Joint Typhoon Warning Center, Pearl Harbor, HI, 109 pp. [Available at www.dtic.mil/dtic/tr/fulltext/u2/a561986.pdf.]

Chen, S. S., W. Zhao, M. A. Donelan, and H. L. Tolman (2013), Directional wind–wave coupling in fully coupled atmosphere–wave–ocean models: Results from CBLAST-hurricane, *J. Atmos. Sci.*, *70*, 3198–3215.

Collins, C. O., III, B. Lund, R. Ramos, W. M. Drennan, and H. C. Graber (2014a), Wave measurement inter-comparison and platform evaluation during the ITOP (2010) experiment, *J. Atmos. Oceanic Technol.*, *31*, 2309–2329, doi:10.1175/JTECH-D-13-00149.1.

Collins, C. O., III, B. Lund, R. T. Waseda, and H. C. Graber (2014b), On recording sea surface elevation with accelerometer buoys: Lessons from ITOP (2010), *Ocean Dyn.*, *64*, 895–904, doi:10.1007/s10236-014-0732-7.

D'Asaro, E. A., et al. (2014), Impact of typhoons on the ocean in the Pacific, *Bull. Am. Meteorol. Soc.*, *95*, 1405–1418, doi:10.1175/BAMS-D-12-00104.1.

Drennan, W. M., and L. K. Shay (2006), On the variability of the fluxes of momentum and sensible heat, *Boundary Layer Meteorol.*, *119*, 81–107, doi:10.1007/s10546-005-9010-z.

Drennan, W. M., J. A. Zhang, J. R. French, C. McCormick, and P. G. Black (2007), Turbulent fluxes in the hurricane boundary layer. Part II: Latent heat flux, *J. Atmos. Sci.*, *64*, 1103–1115, doi:10.1175/JAS3889.1.

Drennan, W. M., H. C. Graber, C. O. Collins III, A. Herrera, H. Potter, R. J. Ramos, and N. J. Williams (2014), EASI: An air–sea interaction buoy for high winds, *J. Atmos. Oceanic Technol.*, *31*, 1397–1409, doi:10.1175/JTECH-D-13-00201.1.

Fisher, E. L. (1958), Hurricanes and the sea-surface temperature field, *J. Meteorol.*, *15*, 328–333.

Geernaert, G. L., K. B. Katsaros, and K. Richter (1986), Variations of the drag coefficient and its dependence on sea state, *J. Geophys. Res.*, *91*, 7667–7679, doi:10.1029/JC091iC06p07667.

Geernaert, G. L., F. Hansen, M. Courtney, and T. Herbers (1993), Directional attributes of the ocean surface wind stress vector, *J. Geophys. Res.*, *98*, 16,571–16,582, doi:10.1029/93JC01439.

Grachev, A. A., C. W. Fairall, J. E. Hare, J. B. Edson, and S. D. Miller (2003), Wind stress vector over ocean waves, *J. Phys. Oceanogr.*, *33*, 2408–2429, doi:10.1175/1520-0485(2003)033<2408:WSVOOW>2.0.CO;2.

Högström, U., et al. (2008), Momentum fluxes and wind gradients in the marine boundary layer – A multi-platform study, *Boreal Environ. Res.*, *13*, 475–502.

Holthuijsen, L. H., M. D. Powell, and J. D. Pietrzak (2012), Wind and waves in extreme hurricanes, *J. Geophys. Res.*, *117*, C09003, doi:10.1029/2012JC007983.

Kuik, A. J., G. P. vanVledder, and L. H. Holthuijsen (1988), A method for the routine analysis of pitch-and-roll buoy wave data, *J. Phys. Oceanogr.*, *18*, 1020–1034, doi:10.1175/1520-0485(1988)018<1020:AMFTRA>2.0.CO;2.

Large, W. G., and S. Pond (1981), Open ocean momentum flux measurements in moderate to strong winds, *J. Phys. Oceanogr.*, *11*, 324–336, doi:10.1175/1520-0485(1981)011,0324:OOMFMI.2.0.CO;2.

Lee, C.-Y., and S. S. Chen (2014), Stable boundary layer and its impact on tropical cyclone structure in a coupled atmosphere–ocean model, *Mon. Weather Rev.*, *142*, 1927–1944, doi:10.1175/MWR-D-13-00122.1.

Longuet-Higgins, M. S., D. E. Cartwright, and N. D. Smith (1963), Observations of the directional spectrum of sea waves using the motions of a floating buoy, in *Ocean Wave Spectra: Proceedings of a Conference*, pp. 111–136, Prentice-Hall, New Jersey.

Monin, A. S., and A. M. Obukhov (1954), Basic laws of turbulent mixing in the surface layer of the atmosphere, *Tr. Geofiz. Inst. Akad. Nauk SSSR*, *151*, 163–187.

Moon, I. J., I. Ginis, and T. Hara (2004), Effect of surface waves on air-sea momentum exchange. Part II: Behavior of drag coefficient under tropical cyclones, *J. Atmos. Sci.*, *61*(19), 2334–2348, doi:10.1175/1520-0469(2004)061<2334:EOSWOA>2.0.CO;2.

Ooyama, K. (1969), Numerical simulation of the life cycle of tropical cyclones, *J. Atmos. Sci.*, *26*(642), 3–40, doi:10.1175/1520-0469(1969)026<0003:NSOTLC>2.0.CO;2.

Potter, H. (2015), Swell and the drag coefficient, *Ocean Dyn.*, *65*(3), 375–384, doi:10.1007/s10236-015-0811-4.

Potter, H., H. C. Graber, N. J. Williams, C. O. Collins III, R. J. Ramos, and W. M. Drennan (2015), In situ measurements of momentum fluxes in typhoons, *J. Atmos. Sci.*, *72*, 104–118, doi:10.1175/JAS-D-14-0025.1.

Powell, M. D., P. J. Vickery, and T. A. Reinhold (2003), Reduced drag coefficient for high wind speeds in tropical cyclones, *Nature*, *422*(6929), 279–283.

Price, J. F. (1981), Upper ocean response to a hurricane, *J. Phys. Oceanogr.*, *11*, 153–175, doi:10.1175/1520-0485(1981)011<0153:UORTAH>2.0.CO;2.

Quanduo, G., and G. Komen (1993), Directional response of ocean waves to changing wind direction, *J. Phys. Oceanogr.*, *23*, 1561–1566, doi:10.1175/1520-0485(1993)023<1561:DROOWT>2.0.CO;2.

Reichl, B. G., T. Hara, and I. Ginis (2014), Sea state dependence of the wind stress over the ocean under hurricane winds, *J. Geophys. Res. Oceans*, *119*, 30–51, doi:10.1002/2013JC009289.

Rieder, K. F., J. A. Smith, and R. A. Weller (1994), Observed directional characteristics of the wind, wind stress, and surface waves on the open ocean, *J. Geophys. Res.*, *99*(C11), 22,589–22,596, doi:10.1029/94JC02215.

Smith, S. D. (1980), Wind stress and heat flux over the ocean in gale force winds, *J. Phys. Oceanogr.*, *10*, 709–726, doi:10.1175/1520-0485(1980)010<0709>WSAHFO.2.0.CO;2.

Smith, S. D., et al. (1992), Sea surface wind stress and drag coefficients: The HEXOS results, *Boundary Layer Meteorol.*, *60*, 109–142, doi:10.1007/BF00122064.

Sreenivasan, K. R., A. J. Chambers, and R. A. Antonia (1978), Accuracy of moments of velocity and scalar fluctuations in the atmospheric surface layer, *Boundary Layer Meteorol.*, *14*, 341–359, doi:10.1007/BF00121044.

Withee, G. W., and A. Johnson (1976), Data report: Buoy observations during Hurricane Eloise (September 19 to October 11, 1975), US Dep. Commer., NOAA, NSTL Station, Mississippi.

Zemba, J., and C. A. Friehe (1987), The marine atmospheric boundary layer jet in the Coastal Ocean Dynamics Experiment, *J. Geophys. Res.*, *92*(C2), 1489–1496, doi:10.1029/JC092iC02p01489.

Zhang, F. W., W. M. Drennan, B. K. Haus, and H. C. Graber (2009), On wind-wave-current interactions during the Shoaling Waves Experiment, *J. Geophys. Res.*, *114*, C01018, doi:10.1029/2008JC004998.

Zhang, J. (2007), An airborne investigation of the atmospheric boundary layer structure in the hurricane force wind regime, Open Access Dissertations. Paper 15, scholarlyrepository.miami.edu/oa_dissertations/15.

Zhang, J. A., and W. M. Drennan (2012), An observational study of vertical eddy diffusivity in the hurricane boundary layer, *J. Atmos. Sci.*, *69*, 3223–3236, doi:10.1175/JAS-D-11-0348.1.